Engineering a Light-Attenuating Artificial Iris

Farah J. Shareef,[1] Shan Sun,[1] Mrignayani Kotecha,[1] Iris Kassem,[2,3] Dimitri Azar,[1,2] and Michael Cho[1,4]

[1]Department of Bioengineering, University of Illinois at Chicago, Chicago, Illinois, United States
[2]Department of Ophthalmology and Visual Sciences, University of Illinois at Chicago, Chicago, Illinois, United States
[3]Medical College of Wisconsin Eye Institute, Milwaukee, Wisconsin, United States
[4]Department of Bioengineering, University of Texas at Arlington, Arlington, Texas, United States

Correspondence: Michael Cho, 500 UTA Boulevard, Suite 226, Arlington, TX 76019, USA; michael.cho@uta.edu.

Submitted: May 20, 2015
Accepted: February 24, 2016

Citation: Shareef FJ, Sun S, Kotecha M, Kassem I, Azar D, Cho M. Engineering a light-attenuating artificial iris. *Invest Ophthalmol Vis Sci*. 2016;57:2195–2202. DOI:10.1167/iovs.15-17310

Purpose. Discomfort from light exposure leads to photophobia, glare, and poor vision in patients with congenital or trauma-induced iris damage. Commercial artificial iris lenses are static in nature to provide aesthetics without restoring the natural iris's dynamic response to light. A new photo-responsive artificial iris was therefore developed using a photochromic material with self-adaptive light transmission properties and encased in a transparent biocompatible polymer matrix.

Methods. The implantable artificial iris was designed and engineered using Photopia, a class of photo-responsive materials (termed naphthopyrans) embedded in polyethylene. Photopia was reshaped into annular disks that were spin-coated with polydimethylsiloxane (PDMS) to form our artificial iris lens of controlled thickness.

Results. Activated by UV and blue light in approximately 5 seconds with complete reversal in less than 1 minute, the artificial iris demonstrates graded attenuation of up to 40% of visible and 60% of UV light. There optical characteristics are suitable to reversibly regulate the incident light intensity. In vitro cell culture experiments showed up to 60% cell death within 10 days of exposure to Photopia, but no significant cell death observed when cultured with the artificial iris with protective encapsulation. Nuclear magnetic resonance spectroscopy confirmed these results as there was no apparent leakage of potentially toxic photochromic material from the ophthalmic device.

Conclusions. Our artificial iris lens mimics the functionality of the natural iris by attenuating light intensity entering the eye with its rapid reversible change in opacity and thus potentially providing an improved treatment option for patients with iris damage.

Keywords: artificial iris, iris functionality, photo-response materials, UV activation, polymer NMR spectroscopy

The human iris provides eye color and facial symmetry while serving a central role in maintaining visual input to the retina. Using the sphincter and dilator muscles, the natural iris quickly and dynamically alters the size of the pupil, allowing for a 30-fold change in light transmission to the retina.[1,2] Excessive light exposure associated with diminished pupil constriction can lead to damage of retinal photoreceptor cells causing a decline in vision over time.[3] Congenital iris defects, such as aniridia or iris coloboma, as well as trauma-induced iris defects, are the two main contributors to reduced functionality of the iris.[4,5] Albinism, in which patients lack the melanin pigment that provides opacity to the natural iris, can also create a larger area through which excessive light can enter the eye.[6] The reduced adaptive response of the iris to light may result in photophobia, glare and haloes, double vision, and decreased visual acuity.[7]

Treatment options to alleviate the adverse effects of iris damage are limited to wearing sunglasses, colored contact lenses, or artificial iris intraocular implants. Although not approved by the Food and Drug Administration (FDA), Morcher GmbH (Stuttgart, Baden-Württemberg, Germany), Ophtec BV (Groningen, The Netherlands), and HumanOptics AG (Erlangen, Bavaria, Germany) fixed-diameter artificial iris implants have been used sparingly in the United States under the FDA's compassionate care clause.[8] Morcher's and Ophtec's implants for partial or complete aniridia use a fixed colored disc composed of polymethylmethacrylate (PMMA), a mechanically stiff polymer, which solely blocks peripheral light entering the eye.[9–11] In contrast to the hard polymers used by Morcher and Ophtec, HumanOptics' artificial iris lens is made of a flexible silicone polymer that allows for a smaller incision site.[12] Including an image of a natural iris allows the HumanOptics implant to be used as a cosmetic option to restore or change iris color. However, its fixed pupil size and thus invariable light transmittance fails to dynamically reduce bright light entering the eye.[13,14]

Morcher, Ophtec, and HumanOptics' artificial iris implants have been shown to decrease glare and photophobia as well as increase visual acuity, but postsurgical complications include decentralization due to migration of the implant, inflammation caused by repeated contact with peripheral tissues, and anterior uveitis.[15–17] Additional undesirable effects include secondary glaucoma, myopic shift, and a ghosting phenomenon causing double vision.[18,19] Furthermore, despite their success in reconstructing the shape and color of the natural iris, all three implants have a set pupil diameter and amount of light transmitted, thus lacking the ability to adapt to changes in incident light. One important criterion for improving the

current treatment options would be to provide the flexibility to attenuate the incident light dynamically.

The development of photo-responsive artificial iris implant should mimic the functionality of the natural iris while restoring iris color and shape. A well-designed artificial iris lens would continuously monitor and reversibly decrease the transmission of light based on the incident light intensity. For example, an increased intensity of ambient light would result in increased activation of the photosensitive component, which should absorb and block transmission of a higher percentage of the bright light, thereby protecting the sensitive photoreceptor cells of the retina. To overcome a major limitation of current iris defect treatment options, rapid activation and reversal times of less than 1 minute would be preferred as well as the synthetic and biocompatible lens materials.

Photochromic or photo-responsive materials are activated by light to undergo a change in molecular conformation. This change switches between a colorless more transparent state and colored opaque state associated with decreased light transmission.[20] Photochromic materials have traditionally been used for nonmedical applications, including memory storage systems, semiconductors, and light-based electric switches. In addition, these materials have been proven safe and effective as external ophthalmic devices such as Transition lenses. Incorporating a photo-responsive material encased within a biocompatible inert polymer without leakage provides an improved means of fulfilling the design criteria. In this study, we present a novel artificial iris that combines photochromic and polymer components to create an ophthalmic device that partially mimics the natural iris and can have long-term implant stability in the eye, which is a major advance over current commercial artificial irises.

Materials and Methods

Manufacturing the Artificial Iris

The artificial iris implant was fabricated using a photo-responsive material encased within a polymer matrix. Pellets of Photopia, which contain the photochromic material (5% wt/vol naphthopyran) in polyethylene (Matsui International, Tokyo, Japan) were melted and reshaped using a hot plate and glass press to create annular disks with the following dimensions: 11-mm outer diameter, 4-mm inner diameter, and 150-µm thickness (Fig. 1A). Encasement within a polymer matrix of biocompatible polydimethylsiloxane (PDMS; Sigma-Aldrich Corp., St. Louis, MO, USA) involved spin-coating and curing a 100-µm layer on each side of the Photopia disk to form the artificial iris (Fig. 1B). Spin-coated thickness was reproducible within 5% error. Polydimethylsiloxane is proven to be biocompatible and has been widely used in tissue engineering. An image of the complete artificial iris construct in its photo-activated and inactive states shows the distribution of Photopia within PDMS (Fig. 2). Selection and use of Photopia, which has a distinctive color change from clear to magenta, induces activation and subsequent light attenuation.

Optical Characterization

The optical functionality of the artificial iris in attenuating incident light was determined with a UV/Vis Spectrophotometer (Beckman Coulter, Brea, CA, USA). The percentage of light transmitted through the artificial iris with and without activation by UV light was measured over a range of wavelengths. Setting the wavelength scan to 300 to 750 nm provided attenuation properties for the two primary regions of interest: the UV (300–400 nm) and visible light spectrum (400–700 nm). To quantify the response of the artificial iris to changes in incident light intensity, neutral optical density filters (optical density = 0, 0.3, and 0.6) were placed between the light source and sample in the spectrophotometer. The wavelength of maximal light attenuation was also determined using these scans. Furthermore, kinetic scans at that wavelength (approximately 360 nm) led to quantification of the activation and reversal times for the artificial iris by measuring the time-dependent percent transmission changes. Image quality after incorporation of the artificial iris into the path of light entering the eye was then assessed. A glass slide etched

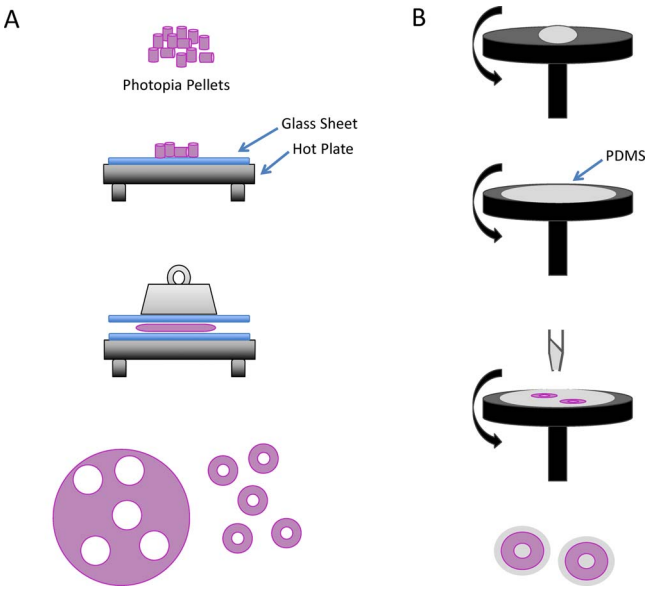

Figure 1. The light-responsive artificial iris was fabricated in two steps: (**A**) photochromic Photopia pellets were heated on a hot plate and reshaped into annular rings using a glass press and cutter, and (**B**) a 100-µm layer of PDMS was spin-coated on each side of the artificial iris to create a disk-shaped construct of 13-mm diameter and 350-µm thickness.

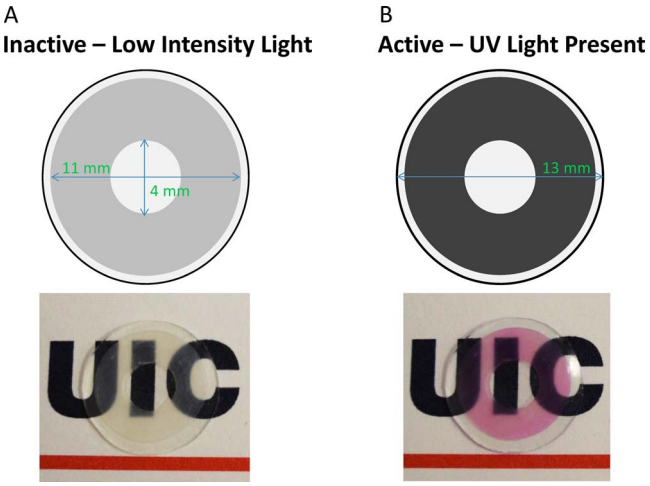

Figure 2. (**A**) Design schematic of artificial iris: the annular dispersion of the photochromic material, Photopia, is shown in *gray*. The *light* and *dark gray* represent the change in color and increased opacity of Photopia on light activation. (**B**) Images of the artificial iris placed on top of the University of Illinois at Chicago (UIC) logo show that visual transparency is maintained with and without activation.

Investigative Ophthalmology & Visual Science

with uniformly spaced lines and a ×10 microscope objective were used to represent the object and lens in a classic image formation. Broadening for the thickness of the lines (e.g., blurring) after placement of the artificial iris between the glass slide and objective then served as a measure to quantify the light scattering expected after implantation.

In Vitro Toxicity Testing

Primary human corneal fibroblasts (HCFs), passage 14 to 16, were cultured in Dulbecco's modified Eagle's medium (Sigma-Aldrich Corp.) supplemented with 10% fetal bovine serum (Atlanta Biologicals, Flowery Branch, GA, USA) and 1% antibiotic-antimycotic solution (Sigma-Aldrich Corp.). Human corneal fibroblasts were seeded on 22 × 22-mm coverslips at a cell density of 20,000 cells per coverslip. Indirect cytotoxicity experiments in which HCFs were exposed to media containing the engineered devices were conducted. In these tests, a glass coverslip seeded with HCFs was placed on top of a Photopia disk without encasement or the artificial iris in a Petri dish filled with media. A live-dead cell viability assay (Invitrogen, Carlsbad, CA, USA) was used to stain cells at days 1, 5, and 10. Experiments consisted of two samples each of control, Photopia, and the artificial iris. Three fluorescent images were taken of each sample using a confocal microscope. Cell count was obtained using ImageJ software (http://imagej.nih.gov/ij/; provided in the public domain by the National Institutes of Health, Bethesda, MD, USA).

Structural and Chemical Characterization Using ^{13}C NMR

The ^{13}C nuclear magnetic resonance (NMR) experiments were performed to elucidate the chemical composition and stability of Photopia and the artificial iris in aqueous solution. Specifically, we aimed to identify the reactive, and potentially toxic, side chains of Photopia in solution. Photopia and artificial iris samples immersed in PBS for 3 days were evaluated using ^{13}C NMR along with samples of supernatant PBS exposed for 1 month to Photopia and the artificial iris to determine potential leaching of substances in solution. The NMR measurements were performed using ^{1}H decoupled ^{13}C NMR pulse program (Bruker – zgpg; Billerica, MA, USA) at room temperature on an 8.5-T (^{1}H frequency = 360.13 MHz and ^{13}C frequency = 90.55 MHz) Bruker Advance spectrometer equipped with a quadruple nucleus probe capable of multinuclear NMR measurements. A capillary filled with D_2O was placed in the NMR tube to achieve magnetic field homogeneity over the sample volume by locking the deuterium signal. The solid Photopia and artificial iris samples in PBS were placed on top of a doty aurum plug (14 mm) to keep the samples at the center of the radiofrequency coil. The 90° pulse width was 8.75 μs for the monomer solutions and was used as is for polymer samples. The relaxation delay was set to 2 seconds and the number of scans to 1024. The experimental parameters for supernatant samples were the following: 90° pulse width = 13.5 μs, relaxation delay = 2 seconds, and number of scans = 3072. The dimethyl sulfoxide (DMSO) carbon peak at 39.5 ppm was used for chemical shift reference.

Results

Characterization of Artificial Iris

Activation of Photopia and attenuation of incident light were first established through observation of the distinct color change from clear to magenta in response to UV exposure (see Fig. 2B). Subsequent optical testing to quantify the functionality of the artificial iris demonstrated rapid but not instantaneous activation using UV and blue light with maximal activation achieved in less than 30 seconds (images not shown). Similarly, the artificial iris demonstrated gradual reversal that began immediately after removal of the light stimulus with a return to its original state within 1 minute. Wavelength scans of the artificial iris showed maximal attenuation at 390 nm with more than 60% of incident UV light (300–400 nm) and 50% to 65% of visible light (400–700 nm) blocked (Fig. 3A). It was also noted that the artificial iris attenuated a larger percentage of visible light in the green to orange (450–650 nm) range when preactivated by UV light exposure for 30 seconds (Fig. 3A, UV-activated artificial iris). The maximum attenuation (i.e., maximum absorbance) was found to occur at 390 nm. This coincides with the required energy to reversibly break a carbon-oxygen bond in Photopia and thus allowing optical modulation of transmitted light. Characterization of the artificial iris's response to changes in incident light intensity was achieved using neutral density filters of optical density 0, 0.3, and 0.6 to modulate the intensity of incident light by 0%, 50%, and 75%, respectively. It was designed to create varying ambient light intensity environments. The percentage of light blocked by the artificial iris at a given intensity was calculated by taking the difference between the incident light on the artificial iris after traversing the neutral density filter and the percent of that light transmitted through the artificial iris. As the optical density of the filters increases (i.e., the intensity of the light on the artificial iris decreases), the percentage of that incident light blocked by the artificial iris also decreases from 60% to 10% (Fig. 3B). In other words, as the incident light becomes dimmer, the artificial iris transmits more light, thereby attenuating high-intensity light while ensuring enough light enters the eye in the low light intensity environment.

Experiments to assess postimplant image quality were conducted using a glass slide etched with uniformly spaced lines 100 μm apart and a ×10 microscope objective to represent an object-lens-image visual system. The control image of the glass slide was acquired using differential interference contrast microscopy (Fig. 4A). Placement of the annular photochromic region of the artificial iris between the glass slide and the objective resulted in a darkened image (overall pixel intensity was reduced as seen by a gray background compared with the control image) with blurred lines (Fig. 4B). The degradation of image quality is perhaps best characterized by estimating the full width half maximum (FWHM) values. For example, the FWHM was calculated 5 μm in the control experiment without introducing the artificial iris in the optical pathway. This value can be used to represent the resolution and appears to be independent of the wavelength range in this study. Insertion of the artificial iris increased the FWHM by approximately 10-fold to 50 μm. An adjustment of the focal length by approximately 150 μm seemed to reverse the blurring effect (FWHM = 8 μm), resulting in an image of sharply refocused lines with decreased overall pixel intensity (Fig. 4C). The change in resolution of the lines in the three images and the corresponding pixel intensity modulation along a horizontal line are shown in Figure 4D.

In Vitro Response

Human corneal fibroblasts with indirect contact to the artificial iris or Photopia over a 10-day period were stained with green calcein AM (fluorescence green) to identify live cells and ethidium homodimer to highlight the dead cells (red fluoresces red). The resulting images indicate that the viability and proliferation of cells exposed to the artificial iris were

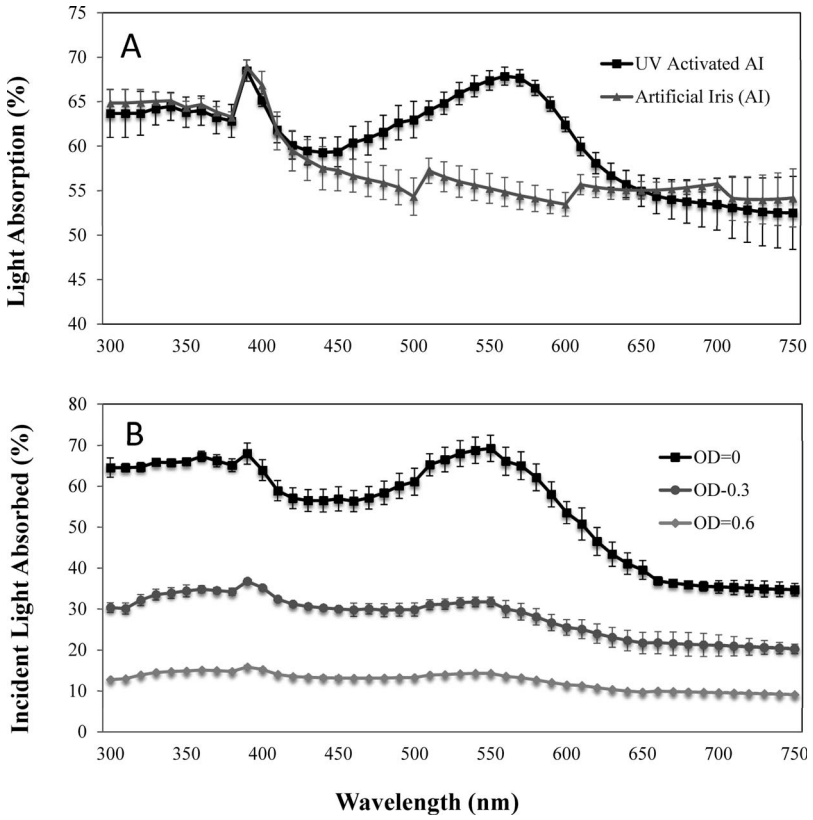

FIGURE 3. (A) Light transmittance of the artificial iris in the ultraviolet (300–400 nm) and visible (400–700 nm) spectrum. Preactivation by exposure to 365-nm light for 30 seconds (UV activated) results in reduced transmission in the green to orange (450–650 nm) range, thus highlighting the additional light blocked by the artificial iris when outdoors or in the presence of UV light. (B) The percentage of incident light absorbed by the artificial iris increases from 12% to 60% as the intensity of the incident light on the construct is increased. Thus, the artificial iris has higher light attenuation in bright light than it does in dim light settings.

comparable to those of the control sample (Fig. 5A). However, cells exposed to Photopia alone versus the control sample showed decreased live cells after 5 and 10 days. Quantification of live HCFs from these fluorescent images confirmed no significant difference in the number of live cells between the artificial iris and control samples at day 1 through 10 (Fig. 5B). In contrast, on days 5 and 10, the average live cell count was 40% less for HCFs exposed to Photopia compared with the control.

Structural and Chemical Characterization Using ^{13}C NMR

Following our in vitro experiments, NMR spectroscopy was used to determine Photopia's chemical structure and potentially reactive side groups and to validate the stability of the artificial iris in solution. The ^{13}C NMR spectra of Photopia and the artificial iris immersed in PBS for 3 days (Fig. 6A) identified the mobile molecular groups in the samples. The assignments are given in the Table. The common peaks seen in these scans belong to Photopia. It was noted that on coating with PDMS, an additional strong peak related to CH_3 of PDMS appears in the artificial iris spectra and the peaks related to Photopia are shifted upfield. A second set of NMR experiments (Fig. 6B) was conducted on PBS exposed to either the artificial iris or Photopia over 1 month to ascertain which molecules if any leached out of the samples over time. For these samples, NMR of the supernatant liquid alone was tested. In the case of no leaching, NMR peaks should not be seen, as there are no carbon-based substances in PBS. However, both the artificial iris and Photopia had CH-O residual monomer peaks, perhaps coming from the main polymer anchor (e.g., CH2 of polyethylene). However, the Photopia sample alone showed an additional peak at 124 ppm possibly coming from the aromatic carbon group in the naphthopyran (Fig. 6C), which might be responsible for the cell death in Photopia (see Fig. 5A). This potential leaching is effectively blocked in the artificial iris, likely due to PDMS coating and therefore improving the overall cell survival.

DISCUSSION

The light-responsive artificial iris was designed as a biocompatible ophthalmic implant with self-adjusting light transmission properties to partially mimic the functionality of the natural iris. Dynamic light attenuation was achieved through incorporation of a photo-responsive material (Photopia, 5% naphthopyran) that undergoes a reversible molecular conformational change induced by UV or blue light.[21] Photochemical cleavage of the carbon-oxygen bond within the pyran ring by incident light converts a naphthopyran to its colored opaque ring-open state, while reversal to its original transparent ring-closed form occurs spontaneously with removal of the UV light stimulus.[22] This class of photochromic materials is particularly suited for ophthalmologic applications due to its efficient photo-response, large light absorbance when activated, rapid reversal, and fatigue resistance.[23]

Encasing an annular disk of Photopia within PDMS (Figs. 1, 2) to form the artificial iris implant met our design objectives by restoring iris shape and providing significant light attenu-

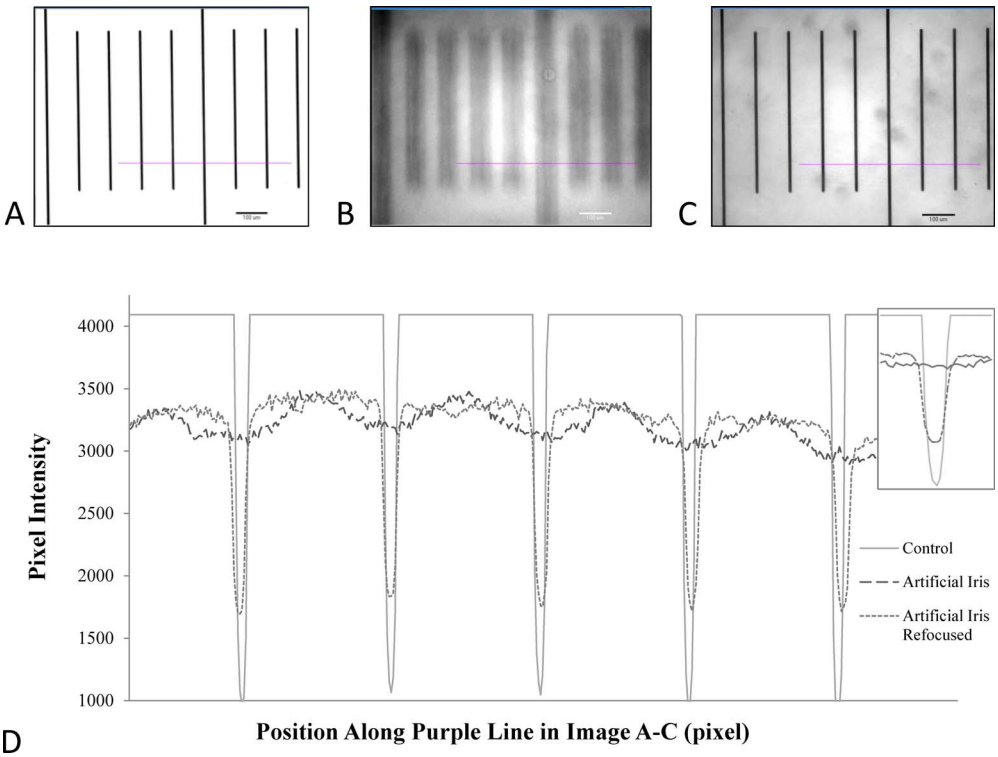

Figure 4. (**A**) Control. Image of glass slide with *black lines*. (**B**) Artificial iris. Image through peripheral photochromic region of artificial iris (AI): light scattering (increased thickness of *blurred black lines*) and decreased overall light transmission (*gray background*). (**C**) Artificial iris refocused. Image through peripheral artificial iris after focal length increased by approximately 150 μm: visual acuity restored. (**D**) Pixel intensity versus position along *purple lines* in (**A**) to (**C**). Image resolution denoted by the full width half maximum of control (**A**) and artificial iris refocused (**C**) is greater than image formed through artificial iris alone (**B**). Reduced light transmission (decreased baseline intensity) for images through AI (**B** and **C**) compared with control (**A**) was also noted.

ation while maintaining visual acuity through the clear center where light passes unimpeded for sight. Through selection of a photo-responsive material with activation and reversal times in less than 1 minute, we have overcome the primary limitation of other iris defect treatment options such as Transition lenses, which have prolonged reversal times in excess of 10 minutes when indoors. Similarly, the use of this particular self-adaptive light-sensitive material resulted in a less bulky alternative to the circuits found in electric artificial irises[24] and improved on current commercial artificial irises, such as HumanOptics AG through its light-attenuating profile.[25] Encasing Photopia in hydrophobic PDMS was central to preventing cell migration and surface attachment, which could affect light transmission through our artificial iris.

The human eye relies on the pupillary light reflex, the constriction and recovery of the iris in response to light stimulus, to modulate the light flux into the eye.[26] Along with controlling retinal illumination, a light-responsive pupil can change the depth of focus and, with a smaller pupil size, reduce optical aberrations, light diffraction, and visual effects such as glare.[27,28] Our goal in engineering a new artificial iris was to restore these natural iris properties to patients with congenital or trauma-induced iris defects. By blocking up to 60% of incident light across the UV and visible light spectra,

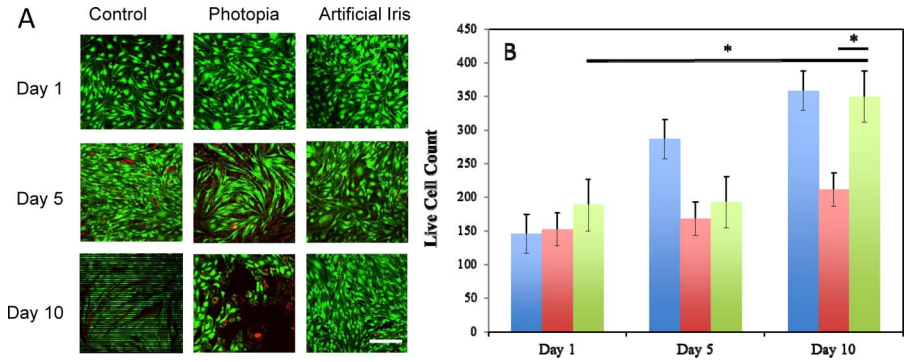

Figure 5. Human corneal fibroblasts were cultured with either the annular Photopia disks or the complete artificial iris for up to 10 days. (**A**) Cell viability staining (live cells = *green*, dead cells = *red*) show similar morphology and proliferation rate between control and artificial iris–exposed HCFs, whereas cell death and detachment (*black areas* represent cell-free regions) was noted for HCFs cultured with Photopia. For all images, *scale bar* = 200 μm as seen in *bottom right image*. (**B**) Quantification of live cells elucidated that Photopia counteracts cell proliferation as live cell count did not significantly change from day 1 to 10. Control, *blue*; Photopia, *red*; artificial iris, *green bars*.

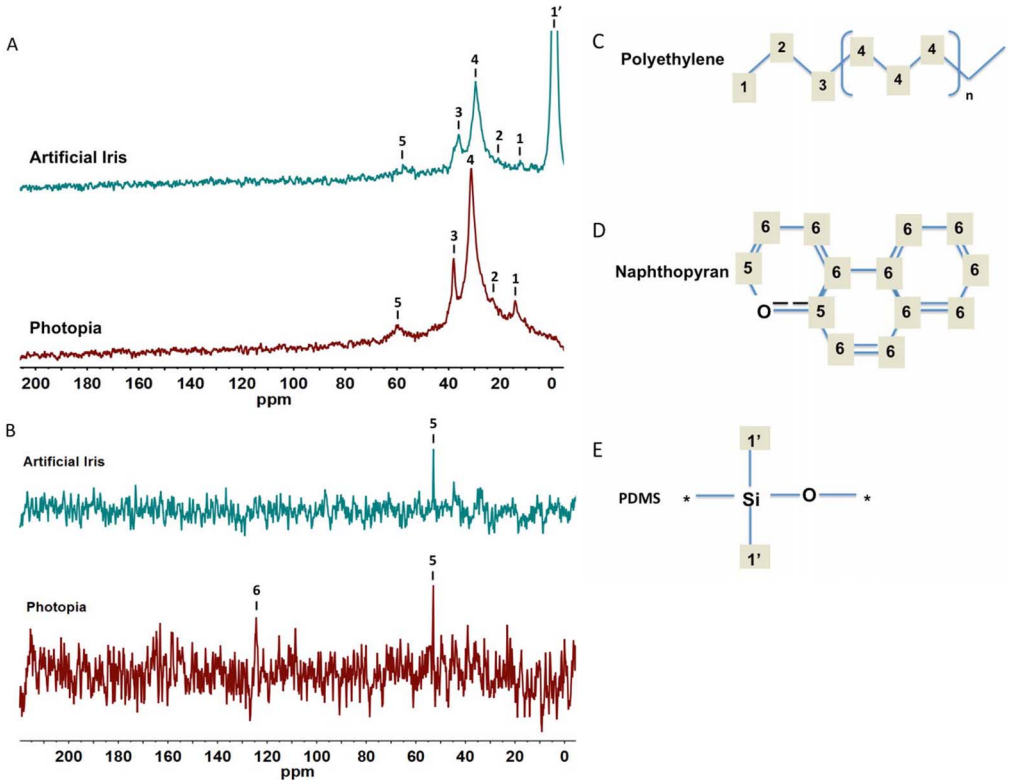

Figure 6. **(A)** ^{13}C NMR spectra of Photopia and artificial iris samples immersed in PBS. The visible peaks are from mobile fractions of polymers in aqueous solution. **(B)** ^{13}C NMR spectra of supernatant PBS exposed to Photopia and artificial iris for 1 month. The 124-ppm peak seen in Photopia supernatant is effectively blocked and not visible in the artificial iris supernatant sample. **(C)** Chemical structure of polyethylene, naphthopyran, and PDMS. The reversible and photoactive C-O bond in naphthopyran is indicated by a *dashed line*.

our artificial iris approaches such a design goal (Fig. 3A, artificial iris). Furthermore, when activated by UV light, the artificial iris blocks an additional 10% of green to orange light (450–650 nm), thereby enhancing its light sensitivity when outdoors or in the presence of harmful UV radiation (Fig. 3A, UV-activated artificial iris).

As the naphthopyran side groups largely determine its light-transmission properties, Photopia's unique chemical structure allows for the increased attenuation of visible light in the active state.[22] In addition to diminishing the amount of light entering the eye based on wavelength, our artificial iris has graded light transmission depending on the intensity of the incident light. Applying neutral-density filters with optical density of 0, 0.3, and 0.6 to alter intensity across the light spectrum showed that as the ambient light brightens, a larger percentage of that light is absorbed (Fig. 3B). Thus, similar to the natural iris, our implantable artificial iris has the sensitivity to inhibit high-intensity light while allowing enough light to enter the eye in dim settings to maintain vision.

Although the artificial iris retains visual acuity through its clear pupillary region, it was hypothesized that the image through the photochromic region may have decreased clarity due to the molecular structure of Photopia. The classic optics model of an object-(artificial iris)-lens-image system was used to characterize the change in visual acuity through the peripheral artificial iris. We found an approximately 25% decrease in the baseline intensity (Fig. 4), which corroborates the results of previous optical testing and confirmed the artificial iris's ability to attenuate incident bright light. We also noted a quantifiable degree of light scattering (Fig. 4D) as indicated by the increased FWHM estimates. However, further testing indicated that adjusting the focal length by 150 μm at which the image through the peripheral artificial iris was taken could counter and minimize this light scattering (Fig. 4C) while providing the expected light attenuation. The graph of pixel intensity verses position along a preselected line (Figs. 4A–C) more clearly demonstrates that changing the focal length can restore image resolution (Fig. 4D). For this graph, the image resolution is depicted by the change in pixel intensity between the white background and the black lines as seen in the control image. In comparison, the artificial iris curve has decreased baseline pixel intensity and a more gradual change in the slope representing the light diffraction of the lines imaged through the peripheral artificial iris. However, the similarity in steepness of the pixel intensity curves for the control and

Table. ^{13}C NMR Chemical Shift and Assignments

	Peak Number	Chemical Shift, ppm	Assignments
Artificial iris	1′	1.02	CH_3 (PDMS)
	1	12.13	CH_3 (PE)
	2	20.9	CH_2 (PE)
	3	29.5	CH_2 (PE)
	4	36	CH_2 (PE)
	5	57.3	CH-O (NTHP)
Photopia	1	14.29	CH_3 (PE)
	2	23.10	CH_2 (PE)
	3	31.28	CH_2 (PE)
	4	37.86	
	5	60.32	CH-O (NTHP)
Artificial iris	1	53.04	CH-O (NTHP)
Photopia	1′	53.04	CH-O (NTHP)
	2′	124	C (NTHP)

artificial iris refocused images signifies that the image degradation can be reversed and corrected with a change in focal length.

Collectively, the visual acuity data indicated that images taken through the periphery of the artificial iris would have reduced pixel intensity but diminished resolution compared with images through the clear PDMS center, unless the focal length was adjusted. Fortunately, simulating a change in focal length (i.e., optical power) to maintain focus on objects as their distance varies is an inherent process of the human lens, termed accommodation.[29] Given that the optical power of the human lens is measured in diopters, calculated as the inverse of focal length, the 150-μm change in focal length required for visual clarity is equal to a change in optical power by 0.55 diopters. As the optical power of the human lens can vary up to 10 diopters or more until age 40, it appears the natural lens could accommodate the light diffraction through the peripheral artificial iris post implant. Thus, individuals with our artificial iris could maintain visual acuity when light passes through both the clear center and the light-responsive peripheral region of the implant.[30]

Once it was determined that our artificial iris met the optical design criteria, we pursued cell culture experiments to ascertain the biocompatibility of the artificial iris in vitro. Human corneal fibroblasts were indirectly exposed to samples of the artificial iris and Photopia alone for up to 10 days. Cell viability was established when normal morphology and proliferation rates were observed for HCFs exposed to the artificial iris compared with control samples (Fig. 5A). The biocompatibility of the artificial iris was then validated when subsequent analysis indicated no significant change in live cell count (Fig. 5B) for artificial iris and control samples at all study time points. In contrast, the decreased number of HCFs in the Photopia samples highlighted the potential adverse effects of exposure to Photopia alone. As the artificial iris consists of Photopia encased in PDMS, a polymer whose biocompatibility has been well established,[31,32] the in vitro data suggested that the design of the artificial iris inhibited cell death despite the possible toxicity of Photopia. We postulate that interaction of ionic media with reactive surface naphthopyran molecules in Photopia might have caused the cell death observed with the Photopia samples.

Based on the in vitro data, we endeavored to determine the molecular structure of Photopia and any potentially reactive side chains that could cause toxicity in solution. In addition, we aimed to ascertain the stability of the artificial iris implant over time. Commonly used to determine the structure and morphology of inorganic materials, NMR spectroscopy detects the chemical environment of atomic nuclei based on the differences in electromagnetic radiation they emit in the presence of a high magnetic field.[33] The mobile molecular groups in both samples were identified using ^{13}C NMR scans of Photopia and the artificial iris in PBS and are shown in the Table. Common peaks between the scans (Fig. 6A) were used to identify the molecular components of Photopia. The upfield shift of the Photopia-related peaks in the artificial iris spectra and the presence of the strong CH_3 peak associated with the PDMS coating indicated that PDMS served as an effective barrier in preventing the interaction of Photopia with the ions in aqueous solution. Another set of NMR experiments (Fig. 6B) on PBS exposed to the artificial iris or Photopia for 1 month was conducted to ascertain if molecular leaching would occur over time. Nuclear magnetic resonance testing of the supernatant liquid alone showed a peak at 124 ppm in the Photopia sample not seen in the artificial iris scan that could have arisen from the aromatic carbon group in the naphthopyran (Fig. 6C). This additional molecular species in solution may explain the cell death seen in images of Photopia at day 10 (see Fig. 5A). Furthermore, it confirms that the PDMS coating in the artificial iris effectively prevents leaching of aromatic carbon group while ensuring in vitro cell survival and stability of the implant over time.

Conclusions

Our light-activated artificial iris is a biocompatible implant that partially mimics the functionality of the natural iris while restoring iris aesthetics. Incorporation of a photo-responsive material encased in a PDMS matrix to engineer our device provides for a new artificial iris design. The dynamic light attenuation based on the ambient light intensity and wavelength (UV or visible light) characteristic of our artificial iris improves on the properties of commercial artificial iris implants. The ability to attenuate up to 60% of incident light provides our artificial iris with the means to alleviate or at least significantly reduce the symptoms of iris damage, such as photophobia, glare, and haloes. By maintaining visual acuity for light traversing both the central transparent PDMS as well as the light-responsive peripheral region, our implant proves comparable to commonly used intraocular lens implants. Unlike photochromic intraocular lenses that filter out UV and blue lights by absorbing them,[34,35] the artificial iris we developed filters and uses UV lights to activate the photo-response materials to dynamically modulate the incident light intensity. In addition to providing enhanced optical properties, it demonstrated biocompatibility in vitro despite potential toxicity from Photopia alone. Follow-up testing using ^{13}C NMR served to identify structural characteristics of Photopia including ones that may lead to toxicity in solution as well as established that the PDMS coating in the artificial iris prevents leaching. Future work on artificial iris implantation in the rabbit eye would be necessary to confirm these findings in vivo. Although the final design of the artificial iris will be optimized based on preclinical animal model studies, we have successfully engineered a photo-responsive and biocompatible artificial iris implant with dynamic light-attenuation properties that may provide a new treatment option for patients with congenital or trauma-induced iris defects.

Acknowledgments

We thank Carlos Ng for his expertise and effort with artificial iris microfabrication.

Supported by the FMC Technologies, Inc., Fellowship (FS), Office of Naval Research Grant N00014-13-1-0404 (MC), National Institutes of Health Grant NEI K08 EY024645 (IK), and National Eye Institute Core Grant P30 EY001792 (IK).

Disclosure: **F.J. Shareef**, None; **S. Sun**, None; **M. Kotecha**, None; **I. Kassem**, None; **D. Azar**, None; **M. Cho**, None

References

1. Watson AB, Yellott JI. A unified formula for light-adapted pupil size. *J Vis*. 2012;12(10):12.
2. Campbell NA. *Biology*. 2nd ed. Menlo Park, CA: Benjamin-Cummings Publishing Company; 1990.
3. Glickman RD. Phototoxicity of the retina: mechanisms of damage. *Int J Toxicol*. 2002;21:473–490.
4. van Heyningen V, Hanson I, Hingorani M. Aniridia. *Eur J Hum Genet*. 2012;20:1011–1017.
5. Brooks BP, Meck JM, Haddad BR, Bendavid C, Blain D, Toretsky JA. Uveal coloboma: clinical and basic science update. *Curr Opin Ophthalmol*. 2006;17:447–470.
6. Brondum-Nielsen K, Grønskov K, Ek J. Oculocutaneous albinism. *Orphanet J Rare Dis*. 2007;2:43–50.

7. Mavrikakis I, Mavrikakis E, Syam PP. Surgical management of iris defects with prosthetic iris devices. *Eye (Lond)*. 2005;19: 205–209.
8. Stephenson M. More appealing options for artificial iris patients. *Rev Ophthalmol*. 2010;17:30.
9. Morcher Implants. Available at: http://www.morcher.com/en.html. Accessed April 7, 2015.
10. Chung M, Miller KM, Weissman BA. Morcher iris reconstruction lens and rigid contact lens for traumatic aniridia. *Eye Contact Lens*. 2009;35:108–110.
11. Ophtec Iris Reconstruction System. Available at: http://www.ophtec.com/. Accessed April 7, 2015.
12. Doran M. Iris implant advance–but face continuing challenges. *EyeNet Magazine*. February 2013:29–31.
13. Human Optics Artificial Iris. Available at: http://www.humanoptics.com/en/. Accessed February 15, 2016.
14. Krader CG. Posterior chamber implant reduces visual problems. *Ophthalmology Times*. 2011;36:24–25.
15. Osher RH, Karatza EC, Burk SE, Snyder ME. Outcomes of prosthetic iris implantation in patients with albinism. *J Cataract Refract Surg*. 2007;33:1763–1769.
16. Olson M, Masket S, Miller KM. Interim results of a compassionate-use clinical trial of Morcher iris diaphragm implantation: report 1. *J Cataract Refract Surg*. 2008;34: 1674–1680.
17. Liu C, Lee RM, Dubois VD, et al. Opaque intraocular lens implantation: a case series and lessons learnt. *Clin Ophthalmol*. 2012;6:545–549.
18. Manero F, Güell JL, Morral M, Gris O, Elies D. Transient myopic shift after phakic intraocular lens implantation. *J Cataract Refract Surg*. 2012;38:1283–1287.
19. Patel CK, Yusuf IH, Arun KS, Rosen P. Black-on-black secondary occlusive IOL implantation to alleviate enigmatic light perception through a black IOL. *J Cataract Refract Surg*. 2013;39:1439–1441.
20. Dürr H, Bouas-Laurent H. *Photochromism: Molecules and Systems*. Amsterdam, The Netherlands: Elsevier Publishing; 2003.
21. Crano JC, Guglielmetti RJ. *Organic Photochromic and Thermochromic Compounds: Volume 1: Main Photochromic Families*. New York: Kluwer Academic Publishers; 2002.
22. Song L, Yang Y, Zhang Q, Tian H, Zhu W. Synthesis and photochromism of naphthopyrans bearing naphthalimide chromophore: predominant thermal reversibility in color-fading and fluorescence switch. *J Phys Chem B*. 2011;115: 14648–14658.
23. Zhen W, Meng Q, Zhang Z, Fu D, Zhang W. Synthesis and photochromic properties of substituted naphthopyran compounds. *Tetrahedron*. 2011;67:2246–2250.
24. Lapointe J, Durette JF, Harhira A, Shaat A, Boulos PR, Kashyap R. A 'living' prosthetic iris. *Eye*. 2010;24:1716–1723.
25. Miller KM, Rosenthal KJ, Snyder ME, Tam DY, Oetting T. Cataract and lost iris tissue after trauma. *Cataract & Refractive Surgery Today*. January 2012:42–46.
26. Winn B, Whitaker D, Elliott DB, Phillips NJ. Factors affecting light-adapted pupil size in normal human subjects. *J Invest Ophthalmol Vis Sci*. 1994;35:1132–1137.
27. Markwell E, Feigl B, Zele AJ. Intrinsically photosensitive melanopsin retinal ganglion cell contributions to the pupillary light reflex and circadian rhythm. *Clin Exp Optom*. 2010;93: 137–149.
28. Mathôt S, van der Linden L, Grainger J, Vitu F. The pupillary light response reveals the focus of covert visual attenuation. *PLoS One*. 2013;8:e78168.
29. Chien C-H, Huang T, Schachar RA. Analysis of human crystalline lens accommodation. *J Biomech*. 2006;39:672–680.
30. Abolmaali A, Schachar RA, Le T. Sensitivity study of human crystalline lens accommodation. *Comput Methods Programs Biomed*. 2007;85:77–90.
31. Bélanger M-C, Marois Y. Hemocompatibility, biocompatibility, inflammatory and in vivo studies of primary reference materials low-density polyethylene and polydimethylsiloxane: a review. *J Biomed Mater Res*. 2001;58:467–477.
32. Worthington KS, Wiley LA, Bartlett AM, et al. Mechanical properties of murine and porcine ocular tissues in compression. *Exp Eye Res*. 2014;121:194–199.
33. Kimura H. Molecular dynamics and orientation of stretched rubber by solid-state 13C NMR. *Polymer Journal*. 2010;42:25–30.
34. Ao M, Chen X, Huang C, et al. Color discrimination by patients with different types of light-filtering intraocular lenses. *J Cataract Refract Surg*. 2010;36:389–395.
35. Zhu X-F, Zou HD, Yu YF, Sun Q, Zhao NQ. Comparison of blue light-filtering IOLs and UV light-filtering IOLs for cataract surgery: a meta-analysis. *PLoS One*. 2012;7:e33013.